

**EXPERIMENTAL AND MULTISCALE FINITE  
ELEMENT ANALYSIS OF PULTRUDED KENAF  
COMPOSITES UNDER COMPRESSIVE IMPACT  
LOAD**

**SAREH AIMAN HILMI BIN ABU SEMAN**

**UNIVERSITI SAINS MALAYSIA**

**2019**

**EXPERIMENTAL AND MULTISCALE FINITE  
ELEMENT ANALYSIS OF PULTRUDED KENAF  
COMPOSITES UNDER COMPRESSIVE IMPACT  
LOAD**

by

**SAREH AIMAN HILMI BIN ABU SEMAN**

**Thesis submitted in fulfilment of the requirements  
for the degree of  
Doctor of Philosophy**

**July 2019**

## ACKNOWLEDGEMENT

Bismillahirrahmanirrahim. In the name of Almighty Allah S.W.T., Most Gracious, Most Merciful, the grateful thank is only belong to Him. With His Help and Blessings, finally I have completed this thesis. First and foremost, I would like to convey my sincere gratitude and appreciation to my supervisors, Prof. Dr. Zaidi Mohd Ripin and Associate Prof. Dr. Roslan Ahmad for their invaluable assistance, support, guidance and encouragement towards the accomplishment of this PhD program. Their positive outlook, suggestions, constructive criticism and confidence in my research inspired and encouraged me for the accomplishment of this thesis. I would also like to appreciate the support provided by Prof. Dr. Hazizan Md Akil from School of Material Engineering, for the supply of composite materials for experimental testing. I appreciate the role of the academic and technical staff for their various contributions and assistance, directly or indirectly in the running on this project. In addition, I would like to take this opportunity to thanks to my sponsors, Kementerian Pengajian Tinggi (KPT) and Universiti Sains Malaysia which enabled me to follow this PhD program. Finally, this thesis is dedicated to my beloved parents; Mr Abu Seman Bin Sareh Md. Isa and Mrs Norazizan Binti Ismail for their love, encouragement, continual support and prayers throughout my educational endeavours. My special gratitude is due to my wife Azliza Othman and my children, Sareh Aqil Rayhan and Tuanpah Aleesya Aulia for their loving support, understanding and endless love. Without your love and support, I could not have accomplished any of this work. Last but not least, I offer my regards and blessings to those who have directly or indirectly contributed in this research, your kindness means a lot to me.

## TABLE OF CONTENTS

<b>ACKNOWLEDGEMENT</b> .....	<b>ii</b>
<b>TABLE OF CONTENTS</b> .....	<b>iii</b>
<b>LIST OF TABLES</b> .....	<b>xii</b>
<b>LIST OF FIGURES</b> .....	<b>xiii</b>
<b>LIST OF SYMBOLS</b> .....	<b>xx</b>
<b>LIST OF ABBREVIATIONS</b> .....	<b>xxiii</b>
<b>ABSTRAK</b> .....	<b>xxv</b>
<b>ABSTRACT</b> .....	<b>xxvii</b>
<b>CHAPTER 1 INTRODUCTION</b> .....	<b>1</b>
1.1 Background .....	1
1.2 Kenaf fiber as reinforcement material.....	2
1.2.1 Industrial application and markets .....	4
1.3 Problem statements .....	5
1.4 Aim and objectives .....	8
1.5 Research scope .....	9
1.6 Thesis outline .....	10

**CHAPTER 2 LITERATURE REVIEW..... 12**

2.1 Mechanical behavior of kenaf composite material ..... 12

2.2 Impact behavior of kenaf composite materials ..... 14

2.3 Compressive failure of fiber-reinforced composites ..... 15

    2.3.1 Fiber and matrix failures ..... 16

        2.3.1(a) Fiber failure ..... 18

        2.3.1(b) Matrix and fiber/matrix interface failure ..... 24

2.4 Failure of kenaf composite ..... 27

2.5 Microstructural damage examination ..... 30

2.6 General idea and categorization of modelling scale ..... 31

    2.6.1 Micro-scale modelling approach ..... 34

    2.6.2 Meso-scale modelling approach ..... 37

    2.6.3 Macro-scale modelling approach ..... 41

2.7 Modeling damage and failure of composites ..... 45

    2.7.1 Failure criteria approach ..... 45

    2.7.2 Damage mechanics approach ..... 51

    2.7.3 Plasticity modelling ..... 54

    2.7.4 Cohesive zone description ..... 55

2.8	FE modeling of natural fiber reinforced composites.....	59
2.9	The effect of fiber misalignment and arrangement on composite performance.....	62
2.9.1	Fiber alignment effect .....	63
2.9.2	Fiber arrangement effect .....	64
2.10	Fiber misalignment in pultruded composite.....	66
2.11	Summary .....	68
<b>CHAPTER 3 METHODOLOGY.....</b>		<b>72</b>
3.1	Introduction .....	72
3.2	Material and specimen preparation .....	72
3.3	Quasi-static testing .....	75
3.4	Split Hopkinson pressure bar (SHPB) testing .....	77
3.4.1	SHPB with momentum trapping modification.....	78
3.4.2	Calibration of the strain gauge output.....	81
3.4.3	High strain rate experimental procedure .....	83
3.4.4	Signal processing .....	83
3.5	Damage analysis of tested composites .....	87
3.5.1	Scanning electron microscope (SEM) analysis.....	87

3.5.2	Macroscopic analysis .....	87
3.6	Damage evolution monitoring.....	89
3.6.1	High speed image capture .....	89
3.7	Finite element modelling.....	90
3.8	Component material background .....	91
3.9	Micro-scale modelling.....	92
3.9.1	Micro scale unit cell definitions and generation .....	92
3.9.2	Boundary conditions .....	93
3.9.3	Material model .....	97
3.10	Development of a meso-scale model for dynamic kenaf composite analysis with damage and strain rate effect.....	98
3.10.1	Composites geometry.....	98
3.10.2	Determination of fiber dimensions and fiber volume ratio.	100
3.10.3	Modelling procedure of each constituent in the meso-scale structure.....	100
3.10.4	Pure resin matrix modeling .....	100
3.10.5	Fiber tows modelling .....	103
3.10.6	Implementation of the material model in a user material subroutine.....	105

3.10.7	Bonding interface consideration .....	108
3.10.8	Meshing sensitivity .....	109
3.11	Development of a macro-scale model for dynamic kenaf composite analysis with failure criteria and strain rate effect .....	109
3.11.1	Geometry and FE model .....	109
3.11.2	Material properties .....	110
3.11.3	Failure criteria .....	111
3.11.4	Boundary conditions and loadings .....	112
3.11.5	Meshing sensitivity .....	112
3.12	The effect of fiber misalignment and arrangement on predicted stress-strain curve and damage initiation in kenaf composites using meso-scale finite element model .....	113
3.12.1	Fiber misalignment study .....	113
3.12.2	Fiber arrangement study .....	113
	3.12.2(a) Generation of idealized/ regular fiber arrays ....	113
	3.12.2(b) Generation of random fiber arrays .....	114
3.13	Summary .....	115
<b>CHAPTER 4 RESULTS AND DISCUSSION .....</b>		<b>116</b>
4.1	Introduction .....	116

4.2	Strain-time response .....	116
4.3	Stress-strain characteristics .....	118
4.4	Effects of strain rate on initial modulus, failure stress, and failure strain .....	121
4.4.1	Compressive modulus .....	121
4.4.2	Maximum stress .....	122
4.4.3	Failure strain .....	124
4.5	Characterization and analysis of damage specimen under dynamic loading .....	125
4.5.1	Macroscopic observations .....	125
4.5.2	Microscopic observations .....	132
4.6	Deformation and damage development assessment of composite materials by high-speed camera .....	137
4.7	Static and dynamic failure process and mechanism .....	138
4.8	Effect of the rate on evolution of the damage (macroscopic analysis)	143
4.9	Mesh sensitivity study of multi-scale finite element models .....	144
4.10	Micro-scale finite element model of kenaf composite .....	147
4.10.1	Matrix dominated loading modes .....	147
4.10.2	Fiber and interface dominated loading modes .....	149

4.11	Meso-scale finite element model of kenaf composite .....	151
4.11.1	Validation of meso-scale FE models .....	151
4.11.2	Comparison of meso-scale model results with experimental findings.....	153
4.11.3	Comparison of high-speed camera images and meso-scale simulation results on deformation and damage development of kenaf composite .....	156
4.11.4	Numerical characterization of damage development.....	157
	4.11.4(a) Relation between stress distribution and damage evolution of kenaf composite meso-scale model under dynamic loading .....	157
	4.11.4(b) Effect of strain rate on evolution of the meso-scale model damage (failure morphologies) .....	162
4.12	Macro-scale finite element model of kenaf composite .....	164
4.12.1	Validation of macro-scale FE model .....	164
4.12.2	Comparison of macro-scale model results with experimental findings.....	165
4.12.3	Comparison of high-speed camera images and macro-scale simulation results on deformation and damage development of kenaf composite .....	167
4.12.4	Numerical characterization of damage development.....	169

4.12.4(a)	Relation between stress distribution and damage evolution of kenaf composite macro-scale model under dynamic loading .....	169
4.12.4(b)	Effect of strain rate on evolution of the macro-scale model damage (failure morphologies) .....	174
4.13	Comparison between the meso-scale heterogeneous composite model and the macro-scale homogeneous composite model .....	175
4.14	Numerical evaluation of fiber misalignment and fiber arrangement effect in kenaf composite using meso-scale finite element model .....	178
4.14.1	Global stress-strain response, strength and effective modulus under axial compression.....	179
4.14.1(a)	Analysis of fiber misalignment effect .....	179
4.14.1(b)	Analysis of fiber arrangement effect .....	182
4.14.2	Damage initiation and damage development .....	184
4.14.2(a)	Analysis of fiber misalignment effect .....	184
4.14.2(b)	Analysis of fiber arrangement effect .....	186
4.15	Summary .....	188
<b>CHAPTER 5 CONCLUSIONS AND FUTURE WORK .....</b>		<b>190</b>
5.1	Conclusion.....	190
5.2	Future work .....	191

**REFERENCES..... 193**

LIST OF PUBLICATIONS

## LIST OF TABLES

	<b>Page</b>
Table 2.1	Failures of kenaf composite under different loading condition .....29
Table 2.2	FE modeling for damage and fracture of natural fiber reinforced composites.....61
Table 3.1	Mechanical properties of the kenaf fiber .....97
Table 3.2	Mechanical properties of the unsaturated polyester resin .....97
Table 3.3	Mechanical properties of the fiber tow ..... 104
Table 3.4	Properties of fiber/matrix interface ..... 108
Table 3.5	Macro-scale model properties of kenaf composite. .... 111

## LIST OF FIGURES

	<b>Page</b>
Figure 1.1	Physical appearance of kenaf .....3
Figure 2.1	Images of (a) unidirectional kenaf fibers, (b) plain weave kenaf fibers, (c) unidirectional kenaf composite and (d) plain weave kenaf composite .....12
Figure 2.2	Illustration of translaminar, intralaminar and interlaminar fracture modes ..... 15
Figure 2.3	Fiber failure modes: (a) Elastic microbuckling; (b) Kinking and (c) Fiber fracture..... 17
Figure 2.4	Matrix and fiber/matrix modes; (a) Longitudinal ply splitting; (b) and (c) Ply splitting in the laminate plane; (d) Shear band formation..... 18
Figure 2.5	Geometry of a kink band.....20
Figure 2.6	Stages of fiber kinking (loaded), (i) elastic domain; (ii) softening domain; (iii) fiber failure domain.....22
Figure 2.7	(a) Low magnification of a crack propagating from right to left, (b) Initial fiber buckling, (c) Initial cracking, (d) Fully developed kink-band.....23
Figure 2.8	Illustration and photography of several ply splitting micro mechanisms .....26
Figure 2.9	Shear bands found in low and high-aspect samples under quasi-static compression.....27
Figure 2.10	Micro, meso and macro-scale modelling .....32
Figure 2.11	Experimental and numerical a) impact force–displacement histories b) impact energy–time histories .....43
Figure 2.12	Stresses on element .....48

Figure 2.13	Forms of the traction-separation law.....	56
Figure 2.14	Traction-separation behavior of the bonding surface.....	57
Figure 2.15	Damaged traction-separation response for cohesive bonding surface .....	57
Figure 2.16	Typical longitudinal cross section of a composite specimen with misalignment angle .....	64
Figure 2.17	Arrangement of fibers in composite a) Hexagonal array b) Square array c) Random array.....	66
Figure 2.18	Edge of pultruded graphite/epoxy composite along the fibers .....	67
Figure 3.1	Flow chart of research methodology.....	73
Figure 3.2	a) Pultrusion machine used to produce samples b) Schematic representation of pultrusion process.....	75
Figure 3.3	Photographs of pultruded kenaf composite.....	75
Figure 3.4	Instron universal testing machine .....	76
Figure 3.5	Stress-strain curves of kenaf composite under quasi-static loading...	77
Figure 3.6	Split Hopkinson pressure bar .....	78
Figure 3.7	a) A schematic of the SHPB with momentum trapping system. b) SHPB with the developed momentum trapping system.....	79
Figure 3.8	a) Signal wave without momentum trapping b) Signal wave with momentum trapping .....	80
Figure 3.9	Strain gages signals from incident and transmitter bars during calibration.....	82
Figure 3.10	Stresses and forces on incident and transmitter bars during calibration.....	82
Figure 3.11	The typical strain waves from the incident and transmission bars. ...	84
Figure 3.12	A specimen sandwiched between incident and transmitted bars .....	85
Figure 3.13	a) Scanning electron microscope b) Sputter coater.....	87
Figure 3.14	Position of high-speed camera and light sources during SHPB test ..	90

Figure 3.15	Multi-scale modelling approach.....	91
Figure 3.16	Micro-scale unit cell geometries a) Full RVE b) Quadrant of RVE ..	92
Figure 3.17	Model representation of an RVE under longitudinal shear loading...	94
Figure 3.18	Six different loading conditions applied on a unit cell .....	96
Figure 3.19	FE meshes of meso-scale model of kenaf composite.....	99
Figure 3.20	Material properties calibration .....	101
Figure 3.21	Undamaged and damaged response of a material .....	102
Figure 3.22	Flowchart of the Vumat implementation. ....	107
Figure 3.23	Finite element mesh of the kenaf composite specimen and compression SHPB setup .....	109
Figure 3.24	Macro-scale model .....	110
Figure 3.25	Diagram of a unit cell of the hexagonal lattice .....	114
Figure 4.1	a) The typical strain waves from the incident and transmission bars b) strain rate history .....	118
Figure 4.2	(a) Compressive stress-strain behavior of kenaf composite through fiber direction under quasi-static and high strain rate loading. (b) Deformation regions of kenaf composite under quasi-static loading. (c) Deformation regions of kenaf composite under high strain rate loading.....	121
Figure 4.3	Effect of strain rate on compressive modulus.....	122
Figure 4.4	Effect of strain rate on failure stress .....	124
Figure 4.5	Effect of strain rate on failure strain .....	125
Figure 4.6	Fractured specimens under quasi-static compression loading a) kenaf composite b) jute composite.....	127
Figure 4.7	Buckled and fractured fibers due to brooming damage. ....	128
Figure 4.8	a) Schematic orientation of kenaf composite with respect to loading direction b) Front and side views of fractured specimens	

	under different high strain rate loading i) $1500\text{s}^{-1}$ ii) $2000\text{s}^{-1}$ iii) $2500\text{s}^{-1}$ .....	129
Figure 4.9	Kink band formation damage in a) kenaf/unsaturated polyester b) flax-PP/MAPP c) jute-PP/MAPP.....	131
Figure 4.10	Tensile and compressive stress regions generated by buckled fibers.....	132
Figure 4.11	a) Schematic of the area on specimens where SEM images were taken. b) Damage area on lower surface of kenaf composite specimen tested quasi-statically. ....	133
Figure 4.12	a) Schematic of the area on specimens where SEM images were taken. b) Damage area on front surface of kenaf composite specimen tested under high strain rate loading. i) $1500\text{s}^{-1}$ ii) $2000\text{s}^{-1}$ iii) $2500\text{s}^{-1}$ .....	136
Figure 4.13	High-speed photographs of the dynamic failure and fracture process of a kenaf composite specimen at four different stages during an SHPB test under strain rate of $2500\text{s}^{-1}$ . The four stages (a-d) are indicated in the stress-strain curve. ....	138
Figure 4.14	Two forms of ply splitting that develops transverse to the fibers ....	142
Figure 4.15	Fiber fracture found on the fractured kenaf composite specimen....	143
Figure 4.16	Material macroscopic damage, $D_{\text{macro}}$ as a function of the strain rate .....	144
Figure 4.17	Compressive stiffness vs. number of elements in a micro-scale unit cell.....	145
Figure 4.18	Relative percentage difference between predicted and measured compressive strength vs. number of elements in the meso-scale model.....	146
Figure 4.19	Relative percentage difference between predicted and measured compressive strength vs number of elements in the macro-scale model.....	147

Figure 4.20	Stress-strain curves for kenaf composite micro scale unit cell in transverse loading.....	148
Figure 4.21	Stress distribution of micro scale unit cell in (a) transverse tension, (b) transverse compression, (c) transverse shear.....	148
Figure 4.22	Stress-strain curves for kenaf composite micro scale unit cell in longitudinal loading, .....	150
Figure 4.23	Stress distribution of micro scale unit cell in (a) longitudinal tension, (b) longitudinal compression, and (c) longitudinal shear. ..	151
Figure 4.24	Comparison of incident and transmitted strain waves obtained from SHPB and meso-scale model. ....	152
Figure 4.25	The engineering stress-strain curves of kenaf composite, at three different strain rates obtained from simulations and experiments. ..	154
Figure 4.26	Comparison of failure stress and failure strain at three different strain rates obtained from simulations and experiments.....	155
Figure 4.27	Comparison of meso-scale modelling results with high-speed photographs on the fracture process of kenaf composite under strain rate of $2500\text{s}^{-1}$ .....	157
Figure 4.28	Stress history for the meso-scale whole structure composite FEA model under compressive impact loading at the rate of 2000/s. (1) 3D unidirectional fiber reinforcement, (2) matrix.....	160
Figure 4.29	Stress-strain plots with photo events.....	161
Figure 4.30	Failure morphologies I) of fractured specimens and II) of FE meso-scale models at various strain rates. a) $1500\text{s}^{-1}$ b) $2000\text{s}^{-1}$ c) $2500\text{s}^{-1}$ .	163
Figure 4.31	Comparison of incident and transmitted strain waves obtained from SHPB and FE macro-scale model. ....	165
Figure 4.32	The engineering stress-strain curves of kenaf composite, at three different strain rates obtained from macro-scale simulations and experiments. ....	166

Figure 4.33	Comparison of failure stress and failure strain at three different strain rates obtained from macro-scale simulations and experiments. ....	167
Figure 4.34	Comparison of macro-scale modelling results with high-speed photographs on the fracture process of kenaf composite under strain rate of $2500\text{s}^{-1}$ .....	169
Figure 4.35	Stress history for the macro-scale whole structure composite FE model under compressive impact loading at the rate of $2000/\text{s}$ . ....	172
Figure 4.36	Stress-strain curves with photo events .....	173
Figure 4.37	Direction of maximum principal stress in the macro-scale model of kenaf composite .....	173
Figure 4.38	Failure morphologies I) of fractured specimens and II) FE macro-scale model at various strain rates. a) $1500\text{s}^{-1}$ b) $2000\text{s}^{-1}$ c) $2500\text{s}^{-1}$ ... ..	175
Figure 4.39	Side view comparison of fractured specimens of kenaf composite predicted using FE modelling and experimental. a) Macro-scale model b) meso-scale model c) experimental.....	176
Figure 4.40	Top view comparison of fractured specimens of kenaf composite predicted using FE modelling and experimental. a) Macro-scale model b) meso-scale model c) experimental.....	178
Figure 4.41	Stress-strain curves of meso-scale model reinforced with aligned and misaligned fibers. ....	180
Figure 4.42	Shear stress distribution in meso-scale model with a) aligned fiber and b) misalign fiber. ....	181
Figure 4.43	Stress-strain curves of meso-scale model reinforced with hexagonal and random fibers arrangement. ....	183
Figure 4.44	Shear stress distribution in meso-scale model with a) hexagonal arrangement and b) random arrangement. ....	184
Figure 4.45	Fiber compressive failure a) Front view and b) back view of meso-scale model with misaligned fiber in hexagonal array.....	185

Figure 4.46	Fiber compressive failure a) Front view and b) back view of meso-scale model with aligned fiber in hexagonal array.....	185
Figure 4.47	a) Kink band formation in meso-scale model with misaligned fiber b) Kink band formation in kenaf composite specimen. ....	186
Figure 4.48	Fiber compressive failure a) Front view and b) back view of meso-scale model with random fiber arrangement.....	188

## LIST OF SYMBOLS

$\alpha, \beta, \gamma, \phi$	Angle parameters
$\sigma$	Stress
$E_2$	Transverse Young's modulus
$G_{12}$	In-plane shear modulus
$c$	Wave velocity
$E$	Young's modulus
$\rho$	Density
$\ell$	Length
$D$	Diameter
$\varepsilon_I, \varepsilon_R, \varepsilon_T$	Incident, reflected and transmitted strain
$A$	Sectional area
$dx$	Differential element
$t$	Time
$v$	Particle velocity
$f, g$	Arbitrary functions
$\dot{\varepsilon}$	Strain rate
$F$	Force
$x, y, z$	Coordinate axes
$u, v, w$	Displacement in $x, y, z$ Coordinate axes
$\nu$	Poisson's ratio
$X$	Compressive strength

$V_f$	Volume fraction of fibers
$w_f$	Weight of fibers
$w_m$	Weight of matrix
$\rho_f$	Density of fibers
$\rho_m$	Density of matrix
$\bar{\varepsilon}^{pl}$	Equivalent plastic strain
$\eta^+, \eta^-$	Stress triaxiality in uniaxial tensile and compressive deformation state
$p, q$	Pressure and Mises equivalent stress
$\dot{\bar{\varepsilon}}_D^{pl}$	Equivalent plastic strain rate
$\omega_D, \omega_s$	State variable
$\varepsilon_c$	Fracture strain
$\tau_{\max}$	Maximum shear stress
$k_s, k_0$	Material parameter
$\varepsilon_T^+, \varepsilon_T^-$	Equivalent plastic strain at ductile damage initiation for uniaxial tensile and compressive deformation
$\sigma_{eq}$	Equivalent stress
$D$	Damage variable
$\bar{\sigma}_{ij}$	Undamaged effective stress tensor
$d_{ft}, d_{fc}$	Fiber tension and compression damage variables
$d_{mt}, d_{mc}$	Matrix damage variables
$X_{1t}, X_{1c}, X_{2t}, X_{2c}$	Tensile and compressive strength in direction 1 and 2

$S_{ij}$	Failure shear strength in i-j plane
$C_{ij}, C_{ij}^0$	Damaged and undamaged elastic constants
$K_{nn}, K_{ss}, K_{tt}$	Normal, shear and tangential stiffness components
$t_n, t_s, t_t$	Normal, shear and tangential traction stress vector
$G_n, G_s, G_t$	Work done by traction and its conjugate in normal, first and second shear directions
$\sigma_k$	Current yield stress
$\varepsilon_I, \varepsilon_R$ and $\varepsilon_T$	Incident, reflected, and transmitted strains measured in SHPB
$F(J_2)$	Yield function

## LIST OF ABBREVIATIONS

1D	One-dimensional
2D	Two-dimensional
3D	Three-dimensional
ASR	Average strain rate
BPO	Benzoyl peroxide
CaCO <sub>3</sub>	Calcium carbonate
CDM	Continuum damage mechanics
CZM	Cohesive zone model
FEA	Finite element analysis
FEM	Finite element method
KFRC	Kenaf fiber reinforced composite
MAPP	Maleic Anhydride grafted Polypropylene
MARDI	Malaysian Agricultural Research and Development Institute,
MDF	Medium density fiberboard
NFC	Natural fiber composite
NFRC	Natural fiber reinforced composite
PLA	Poly lactide
PLLA	Poly (l-lactic acid)
RUC	Representative unit cell
RVC	Repeated volume cell
RVE	Representative Volume Element
SEM	Scanning electron microscopy

SHPB	Split Hopkinson pressure bar
TEM	Transmission electron microscopy
UCS	Ultimate compressive strength
UD	Unidirectional
VUMAT	Vectorized user-defined material
WWFE	Worldwide Failure Exercise

# **EKSPERIMEN DAN ANALISIS UNSUR TERHINGGA PELBAGAI SKALA KOMPOSIT KENAF PULTRUSI TERHADAP BEBAN IMPAK MAMPATAN**

## **ABSTRAK**

Komposit semulajadi dikenali kerana kualiti ekologi seperti terbiodegradasi, ringan dan boleh diperbaharui. Perubahan iklim global dan pelepasan gas rumah hijau telah mendorong penglibatan komposit semulajadi dalam struktur utama yang menanggung beban. Oleh itu, analisis terperinci tindak balas struktur dan ramalan kerosakan diperlukan untuk penilaian keutuhan struktur. Dalam projek penyelidikan ini, kajian eksperimental dan mikroskopik yang meluas telah dijalankan untuk mencirikan sifat mekanikal dan kerosakan komposit kenaf pultrusi pada pelbagai kadar terikan menggunakan teknik bar tekanan terpisah Hopkinson (SHPB) mampatan yang telah diubahsuai dan mesin ujian sejagat (UTM) sementara mikroskop pengimbasan elektron (SEM) digunakan untuk melihat morfologi permukaan sampel yang telah diuji.

Pendekatan pemodelan pelbagai skala yang terdiri daripada model mikro, meso dan makro telah dibangunkan untuk memberikan anggaran berangka perlakuan mekanikal dan mod kegagalan yang diperhatikan dalam komposit bertetulang gentian kenaf pultrusi terhadap bebanan kadar terikan tinggi mampatan. Dalam model ini, kriteria berasaskan Hashin digunakan untuk mengaktifkan kerosakan manakala pendekatan mekanik kerosakan kontinum digunakan untuk meramal perkembangan kerosakan dalam komposit. Permulaan dan perkembangan nyah-ikatan di antara gentian dan matrik dikaji dengan menggunakan elemen-elemen zon kohesif.

Keputusan eksperimen menunjukkan bahawa kegagalan tegasan, kegagalan terikan dan modulus mampatan mempunyai sensitiviti kadar terikan yang berbeza dengan peningkatan kadar terikan. Pasca ujian imbasan mikroskop elektron mendedahkan bahawa mod dan mekanisma kegagalan yang utama untuk komposit kenaf terhadap mampatan satu arah adalah berbeza apabila keadaan bebanan berubah dari kuasi-statik ke dinamik. Hubungan korelasi yang baik dengan purata ralat <2% telah diperolehi antara lengkung tegasan-terikan serta mod kegagalan yang bertanggungjawab untuk kemajuan dan pertumbuhan kerosakan yang diuji secara eksperimen dan yang diperolehi melalui kaedah berangka. Kesan penjajaran dan penyusunan gentian juga dianalisis secara berangka dengan mempertimbangkan keseluruhan sifat yang diramalkan serta kawasan dan corak kerosakan yang mana berbeza-beza disebabkan oleh ketidakstabilan ricih dan jarak relatif antara gentian. Keputusan meyakinkan yang diperolehi dengan model-model ini berguna dalam pembangunan pendekatan-pendekatan ramalan untuk menyediakan aplikasi kadar terikan yang tinggi terutama di industri automotif dan aeroangkasa untuk bahan komposit kenaf.

**EXPERIMENTAL AND MULTISCALE FINITE ELEMENT ANALYSIS OF  
PULTRUDED KENAF COMPOSITES UNDER COMPRESSIVE IMPACT  
LOAD**

**ABSTRACT**

Kenaf natural composites are recognized for ecological qualities such as biodegradability, lightweight and renewable. Due to global climate change and greenhouse gas emissions, it has pushed the engagement of kenaf natural composite in load-bearing primary structures. Hence, detailed analysis of structural responses and prediction of damage are needed for structural integrity valuation. In this research project, an extensive experimental and microscopic study were conducted to characterize the mechanical and damage behavior of pultruded kenaf composites at various strain rates using modified compression split Hopkinson pressure bar (SHPB) and universal testing machine (UTM) techniques meanwhile scanning electron microscope (SEM) was used to capture surface morphology of damaged samples.

A multi-scale modelling approach which consist of micro, meso and macro-scale models are developed to provide a numerical estimate of the response and failure modes observed in unidirectional kenaf fiber reinforced composites under compressive high strain rate loading. In these models, Hashin-based criteria through a user-defined material subroutine (VUMAT) was used for damage initiation while continuum damage mechanics (CDM) approach was employed to predict the damage progression in composite. Initiation and progression of fiber-matrix debonding was studied by employing cohesive zone elements.

The experimental results indicate that the failure stress, failure strain and compressive modulus show different strain rate sensitivity with increasing strain rate.

Post-test scanning electron microscopy reveals that the dominant failure modes and mechanisms in the kenaf composites under uniaxial compression are different as the loading condition changes from quasi-static to dynamic. Good correlation with average error of <2% is obtained between the measured experimental and numerically obtained stress-strain curves as well as failure modes which are responsible for damage development and growth. The effect of fibers misalignment and arrangement are also analyzed numerically by considering the overall predicted properties as well as damage areas and pattern which varies due to shear instability and relative distance between fibers. The promising results obtained with these models can be useful in the development of predictive procedures to provide new high strain rate application especially in automotive and aerospace industries for kenaf composite materials.

# CHAPTER 1

## INTRODUCTION

### 1.1 Background

Biodegradable natural fibers are leading-edge engineering materials for the 21st century and can have significant impact on the materials usage (Gurunathan et al., 2015). Natural fibers are being considered as the main reinforcement substitute for the polymer based composites in order to reduce the reliance upon petroleum established services and products (Herrera-Franco and Valadez-González, 2005; Sahari et al., 2012). The worldwide production of natural fibers like abaca, coir, fax, hemp, jute, kenaf and sisal are projected for over 33 million tons in 2013 (Townsend and Sette, 2016). This shows that the access to natural fibers supply is not really limited.

Natural fibers can be animal, plant and mineral based. Currently, plant fibers is the most used natural fibers for reinforcement of polymer composites (Mohammed et al., 2015). Bast fibers (for example, hemp, flax, wheat straw, jute, and ramie) or leaf fibers (for example, sisal and banana) are commonly utilized natural plant fibers for composite reinforcement. Main positive attributes of the bast fibers are strong and length. There are several ecological benefits when replacing the synthetic fibers with the natural fibers in thermoplastic and thermoset composites which are lesser carbon dioxide emissions and the absorption of carbon dioxide out of the air throughout the growing process (Cabral et al., 2005; Onal and Karaduman, 2009). On top of that, using natural fibers would also create a much healthier working environment for workers as respiratory disorder is the main risk of dealing with the glass fibers (Costa and Orriols, 2012). Some additional advantages are lower in price along with longer tools life and lower maintenance costs as natural fibers are far less abrasive in comparison with synthetic fibers.

Among these natural fibers, kenaf fiber is one of the well-known natural fibers used as a reinforcement in polymer matrix composites. The attractive features of kenaf fibers are it is low cost, lightweight, renewable, biodegradable and high specific mechanical properties (Nishino et al., 2003). However, the main disadvantage of kenaf fibers in composites is the poor compatibility between natural fibers and matrix which can be compensated by incorporating additives (Kim et al., 2011). Various important applications such as sport and construction had been explored to utilize kenaf fiber especially as non-structural parts. The impact loading application such as automotive and aerospace industries have also shown interest in using more natural fiber composites, in order to reduce the weight. However, kenaf composite on dynamic structural applications commercially is still limited if compared to other natural fiber composite (Kamal et al., 2014).

One of the issues of kenaf natural fiber composite is the lacked information in dynamic mechanical properties and damage behavior reported. Also, the lack of finite element modelling procedures to analyze the response and damage behaviors of kenaf composite materials subjected to dynamic loading (Xiong et al., 2018). These issues are in fact, critical deterrents for generalized use of kenaf natural fibers in high strain rate applications. To address this gap, in this research, a detailed analysis of structural responses and identification of damage of kenaf composite are needed experimentally and numerically for structural integrity valuation.

## 1.2 **Kenaf fiber as reinforcement material**

Kenaf is a commercially-available and economical natural fiber reinforced material (Aji et al., 2009). Kenaf is planted in a large scale which majority of them are in Asian countries such as China, India, and Thailand. Kenaf is a plant originated from

India, Pakistan, Indonesia, Japan, Thailand, Vietnam and Malaysia. (Chew et al., 2017). Kenaf has the capability to grow under a different type of climates with a speedy growth in 3 months, into a height of greater than 3m and also a base diameter of 3 to 5 cm (Pickering et al., 2016). Previous research works cited that the growth rate could get to 10 cm/day under optimal climatic situations (Baillie, 2004). According to Mossello et al. (2010), kenaf can be used as a substitute source of fiber for medium-density fiberboard (MDF) and particleboard fabricating. It was reported that kenaf is marketed at £ 240 ~ £ 400 a ton in 2017 (Peças et al., 2018) .

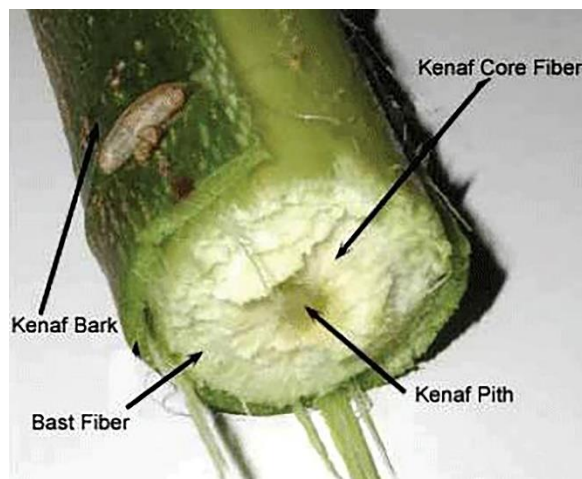


Figure 1.1 Physical appearance of kenaf (Yeong H. Aw, 2004)

Kenaf is a solid and tough plant with a fibrous stalk (Elsaid et al., 2011). The kenaf plant comprises three different kinds of fibers namely bast, core and pith fiber (Karimi et al., 2014) with 35 % bast and 65% core (Khalil et al., 2010) as shown in Figure 1.1. Kenaf bast fibers have remarkable mechanical attributes which made it a good alternative to glass fibers in polymer composites as the reinforcement components (Faruk et al., 2012; Paridah et al., 2011). The mechanical strength and thermal properties of kenaf composite are much greater compared to the other kind of natural fiber polymer composites making it suitable for industrial application (Nishino et al., 2003). Estimated global production of kenaf natural fibers is 0.45 million tons

per year which is on par with flax fibers but much higher than production of hemp, abaca, ramie and sisal fibers which are less than 0.3 million tons per year (Jan, 2009).

### **1.2.1 Industrial application and markets**

Kenaf has turn out to be the substantial natural materials source leading to the evolution of green products in several industries including sports, food packaging and home furniture, cloths, paper pulp, along with fiberboards established businesses (Sanjay et al., 2016; Walther et al., 2007). In Malaysia, Malaysian Agricultural Research and Development Institute, (MARDI) used kenaf polymer composite for building materials and industrial applications, as a commercial interest development (Kamal et al., 2014). The primary cause of this market's growth is the increasing demand for composite materials that are lightweight and ecologically sustainable (Aji et al., 2009). Meanwhile, in the impact loading application such as in automotive industry, the kenaf composite is mostly used as the non-structural parts such as door panel and headliner (Hassan et al., 2017) but rarely been engaged as the load-bearing primary structures. This absent must be due to the impact characteristics and failure behavior of the kenaf composite is not studied in detail and understandable although many investigations have proven that kenaf biocomposite is capable of such applications (Paridah et al., 2008).

The research states that the demand for products using natural fiber reinforcements is growing steadily in the North America which was anticipated to rise by 30% annually for automotive components and 60 percent annually for construction products such as load bearing walls and subflooring. Specifically, the automotive

components such as floor trays and instrumental panels exploit lengthy fibers like flax, jute, hemp, kenaf and sisal (Fogorasi and Barbu, 2017).

In Europe (Kanari et al., 2003) and some Asian countries (Ogushi and Kandlikar, 2005), regulation requires recyclable materials to be part of a vehicle due to concern over automotive end-of-life. By 2006, 80% of the vehicle must be reused or recycled and 85% by 2015. Japan requires the recovery of 95 percent of a vehicle by 2015 (including the burning of certain components). The production of natural fibers (flax, hemp, jute, sisal, etc. excluding wood and cotton) was assessed at 0.36 million metric ton in 2007 and it is expected to reach 3.45 million metric ton in 2020 (Adekomaya et al., 2016). German and Austrian car manufacturers utilized 30 tonnes of natural fibers in producing parts such as seat back, headliner panels and rear and front door panels in 15.7 million passenger cars. Roughly, each car uses 1.9kg of natural fibers composite (Carus et al., 2015).

### 1.3 Problem statements

The increase in environmental consciousness and community interest, the new environmental regulations and unsustainable consumption of petroleum has led to thinking of the use of environmentally friendly materials. Kenaf natural fiber is considered one of the environmentally friendly materials which have good properties over conventional glass and carbon fibers (Saheb and Jog, 1999). The various advantages of kenaf natural fibers over man-made glass and carbon fibers are low cost, low density, comparable specific tensile properties, nonabrasive to the equipment, non-irritation to the skin, reduced energy consumption, less health risk, renewability, recyclability and biodegradability (Nishino et al., 2003). Therefore, kenaf natural fibers have gained the interests of scientists and engineers as a viable alternative for

industrial applications such as for aerospace, leisure, construction, sport, packaging and automotive industries, especially for the last-mentioned application (Anandjiwala and Blouw, 2007).

When designing structural materials for use in different type of applications, effort is directed mainly towards achieving excellent mechanical properties and toughness in the end product giving consideration only to static loading conditions, whilst a similar approach is ignored for dynamic loading conditions. Several studies are available in investigating the responses on natural composites under low velocity impact loadings by using various techniques. Yet, only several researchers have focused on the high strain rate compressive properties of natural composites (Xiong et al., 2018). Under dynamic loading, mechanical properties of materials are known to change, and this places limitations on their performance. Kenaf natural fiber composites have gained growing interest and acceptability as structural material in engineering applications (Anandjiwala and Blouw, 2007). In service, these structures may be subjected to impact loading. Therefore, there is a need to study the dynamic response of kenaf natural fiber reinforced polymer composites and relates the extent of the changes in the mechanical properties to the rate of strain.

Besides mechanical properties characterizations, due to heterogeneous microstructure, natural composites are also characterized by realization of multiple damage modes. Quasi-static and dynamic loading of composite materials result in complex damage mechanisms, in which matrix cracking, tow debonding and fibers fracture are dominant ones. Though damage in composite has been investigated in depth for decades (Liu and Zheng, 2010), the major focus in this study was on the case of unidirectional Kenaf natural fiber reinforced composite under dynamic uniaxial

compressive loads. As a result, research on initiation, progression and interaction of various damage modes in kenaf composite subjected to dynamic loading is limited (Omar et al., 2010; Salman et al., 2016). Further, the behavior of kenaf composites under longitudinal dynamic loading conditions is still to be fully exploited. Therefore, a further research work is needed to investigate and analyze these failure modes under quasi-static and dynamic loads resulting in a better understanding of kenaf behavior.

The inclusion of natural composite materials in engineering applications is clearly on the increase which brings about new challenges for engineers. The composite materials need to go through rigorous, time consuming and expensive experimental impact trials to ensure an adequate level of protection is offered to the structures. This has brought forward the development of computational simulations of the response of composite materials to dynamic loading to reduce the number of experimental trails required and aid in the design process. These simulations, however, are not straightforward and often require a multitude of composite material properties which would normally be obtained from an experimental material characterization program. Multi-scale finite element (FE) modelling has the capability to provide these material properties computationally which would reduce the need for an experimental material characterization test. The applications of this modelling technique for biocomposite materials with a heterogeneous microstructure have been reported previously by a few researchers and there is a growing literature database on the topic (Xiong et al., 2018). However, it has yet to be fully exploited for kenaf fiber composite.

Idealization in the FE analysis can result in errors when the actual fabrication may include fiber misalignment and non-uniform spacing arrangement. Depending on the severity of the fiber misalignment, the difference between actual strength and

stiffness of the composite from the assumed nominal values may become unacceptable or, at least, warrant a reduction of performance expectations. On top of that, there is also some concerns regarding the assumption of the perfect geometry and the ideal tows that will experience "ideal" compression which will contribute to removal of failure modes such as fiber kinking of the tows. Therefore, further research work is needed to develop models that can include these two manufacturing imperfections which has not been applied to unidirectional kenaf composite.

#### 1.4 **Aim and objectives**

The aim of this study is to analyze the mechanical behavior and damage modes of Kenaf fiber reinforced composites under static and dynamic loads using a combination of experimental, microstructural and numerical studies. The following objectives are identified to achieve the aim of this research:

1. To determine the mechanical behavior of kenaf composites under low and high strain rate compression loading.
2. To identify the microstructure of the materials for damage identification using scanning electron microscopy technique.
3. To establish micro, meso and macro-scale FE models to predict the elastic response, damage initiation and evolution of kenaf composite.
4. To provide the areas of stress propagation and stress distribution in dynamically loaded kenaf composite materials using meso and macro-scale FE models.
5. To determine the influence of fiber arrangement and alignment on the effective kenaf composite properties and the induced damage area and pattern using the meso-scale FE models.

## 1.5 Research scope

It consists of two main components: experiments and numerical analysis. The pultruded kenaf composite materials are characterized under static and dynamic load conditions using the universal testing machine (UTM) at  $0.01\text{s}^{-1}$  and modified Split Hopkinson pressure bar technique under strain rate range of 1500 to  $2500\text{s}^{-1}$ . For quasi-static loading,  $0.01\text{s}^{-1}$  was chosen to slowly deform the specimen and thus, the inertia force may be ignored. Meanwhile, high strain rate range between 1500 and  $2500\text{s}^{-1}$  was selected as impact loading applications often occurred in this range or even higher strain ranges (Micallef et al., 2014). Microstructural examination is carried out using the optical microscopy techniques to observe the damage behavior while the high-speed camera is used to record damage sequence. The experimental results are used for finite element model design and validation.

For the finite element analysis, in order to predict elastic response, initiation of damages, evolution of damages and dependency of the strain rate on kenaf composite materials, the multi-scale finite element modelling methodology was established on a micro, meso and macro-scale models. The constituents and fiber/matrix interface were integrated with failure criterion and interface cohesive elements respectively to account for the stiffness degradation and subsequent element removal. The models were then used to determine the zones of stress propagation, stress distribution and mechanical behavior as well as the progressive damage behavior within the kenaf composite. Three different angles of fiber alignment and two fiber arrangements are considered in the study. The angle was selected between  $1-2^{\circ}$  since it was the most common misalignment angle reported for the pultruded parts (Yurgartis, 1987). Meanwhile, random and hexagonal array are chosen as they represent real fibers array of

unidirectional kenaf composites better. All the modeling works are performed using the ABAQUS and Digimat softwares.

## 1.6 Thesis outline

### Chapter 2. Literature Review

A detailed overview of kenaf composite performance, various compressive damage mechanisms are presented in this chapter. A thorough overview of multi-scale modelling approaches and key aspects for predicting damage in composite is given in this chapter. The effect of fiber misalignment and arrangement on the effective composite material properties are also discussed.

### Chapter 3. Methodology (Experimental and numerical modelling)

The first section of this chapter outlines the test methods employed to acquire mechanical properties under dynamic and static conditions, while the second section describes the multi-scale modelling methods for studying deformity and damage of kenaf composite under dynamic loading condition. Last of all, the technique to conduct the fiber misalignment and arrangement studies were explained.

### Chapter 4. Result and Discussion

The first part of this chapter highlights detail of the experimental results of static and dynamic tests and the microstructural damage analysis. The second part describes the numerical results from the multi-scale modelling. Results from meso and macro-scale were also compared for validation. The results from the fiber misalignment and arrangement studies on the effective mechanical properties and developed damage are discussed in detail.

## Chapter 5. Conclusions and Future Work

This chapter presents the results and conclusions derived from the research. Recommendations and suggestions are introduced for potential future research.

## CHAPTER 2

### LITERATURE REVIEW

#### 2.1 Mechanical behavior of kenaf composite material

Mechanical properties variation of kenaf composite are usually based on fibers type, fiber orientation, fibers content, fiber architecture and type of mixer / plasticizer that is used. Example of two different type of kenaf fibers architecture and their composite made up of epoxy matrix are shown in Figure 2.1. The crop growing surroundings, origin region and other features affect natural fiber's shape, size and strength which will affect the mechanical properties (Nishino et al., 2003). Besides, asymmetrical cross sectional area of kenaf fiber also contribute to the variation in the mechanical properties obtained (Terasaki et al., 2009).

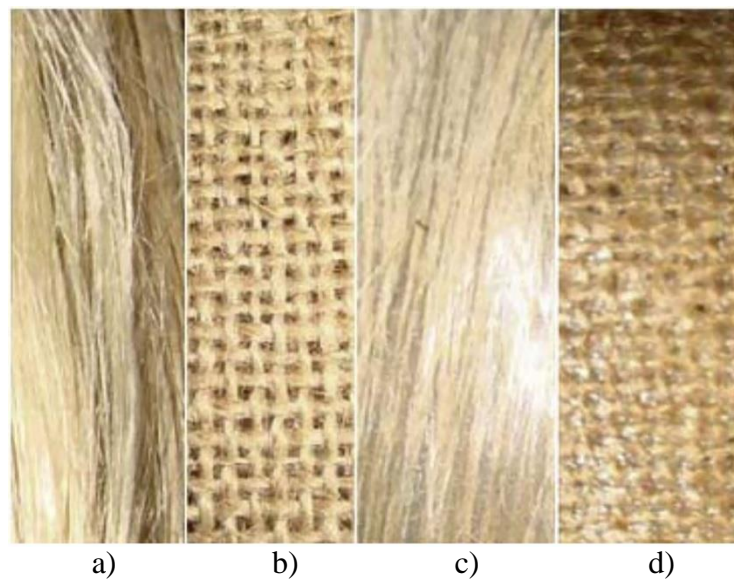


Figure 2.1 Images of (a) unidirectional kenaf fibers, (b) plain weave kenaf fibers, (c) unidirectional kenaf composite and (d) plain weave kenaf composite (Chok. and Majid., 2018; Israr et al., 2019)

Generally, kenaf composite's mechanical properties vary according to kenaf fiber volume exploited. Studies conducted by Nishino et al. (2003) show that the

ultimate tensile strength and Young's modulus increased with the fiber content increase and showed the maximum values when fiber and matrix content are at 70 vol. and 30 vol. percentage respectively (Young's modulus; 6.4 GPa and ultimate tensile strength; 60 MPa). Cultivated from a long rod of kenaf plant which grown under the optimal condition, kenaf fibers reinforced Polylactide (PLA) composites achieve a high increase in tensile and flexural strength of 223 MPa and 254 MPa respectively with 70 percent of fiber volume content (Ochi, 2008).

Effect of different kenaf fiber yarn tex on pultruded kenaf fiber reinforced composites has been studied by Zamri et al. (2016). Comparing to larger tex number, the pultruded composites made with a smaller text number of 1400 show better compressive properties. Smaller tex number contribute to better fiber wetting in composite production and thus increases their characteristics.

Fiber orientation has a significant impact on the mechanical properties of kenaf fiber reinforced composites. The kenaf / Poly (l-lactic acid) (PLLA) composite shows different mechanical properties in directions parallel and perpendicular to a fiber orientation, such as Young's modulus and tensile strength (Nishino et al., 2003).

Incompatibility between natural filler and matrix due to the lignocellulose fiber's inherent polar and hydrophilic nature and polyolefin's nonpolar characteristics made it difficult to blend both materials. To overcome that problems, a specific coupling agent is required such as Maleic Anhydride grafted Polypropylene (MAPP). The effectiveness of MAPP as a coupling agent in kenaf composite has been studied by Sanadi et al. (2001). In comparison with uncoupled composites and unfulfilled Polypropylene (PP), MAPP with the Kenaf-PP composite showed a superior tensile strength of up to 74 MPa.

## 2.2 Impact behavior of kenaf composite materials

The kenaf composite materials are increasingly used as the automotive structures such as bumper and door panel which can be subjected to impact loading (Davoodi et al., 2010). The majority of the studies reported for kenaf composite in dynamic conditions were mostly done using the dynamic mechanical analysis (DMA) and Izod impact test which are dynamic non-destructive material tester and low range strain rate ( $<1000\text{s}^{-1}$ ) impactor respectively. Thus, the experimental studies of the behavior of natural fiber composite especially kenaf composite under high range strain rate conditions ( $>1500\text{s}^{-1}$ ) are still very limited.

Menard (2008) studied the effect of frequency on the value of damping peaks,  $\tan \delta$  max for treated pultruded KFRC and untreated pultruded KFRC using the dynamic mechanical analysis (DMA) technique. The result showed that an increase in frequency has increase the  $\tan \delta$  max values. Dhar Malingam et al. (2018) investigated low-velocity impact properties of woven kenaf reinforced composites using the drop weight impact test. They found that as the impact energy increases, the maximum force has been decreases as well as indentation occurred.

The effect of dynamic loading on the mechanical properties of kenaf composite has been studied by Omar et al. (2010) using the split Hopkinson pressure bar (SHPB). The compression modulus, compressive strength, and 2.5% flow stress of kenaf fiber reinforced polyester composite have increased considerably at an increasing strain rate. Meanwhile, using the Izod impact test, Salman et al. (2016) have studied the effect of impact energy on energy absorption of various kenaf fiber content of woven kenaf composite. The results showed that as the impact energy increases, the energy absorption of kenaf composite with different kenaf fiber content has been increases.

### 2.3 Compressive failure of fiber-reinforced composites

Commonly, compressive failure of fiber-reinforced composite is the consequence of a combination of failure mechanism. Compressive failure is identified with fiber unsteadiness (microbuckling) and matrix yielding, especially in an area where a flaw is available, for example, misaligned fibers or assembling imperfections. Failure modes can be grouped into interlaminar (delamination or separation of plies), intralaminar (in-plane cracks, parallel to fiber direction) and translaminar (cracks perpendicular to fiber direction) fracture as shown in Figure 2.2 (Grove and Smith, 1987). The wide array of local fracture modes and the strong interactions among them are the principal complications for understanding the composite failure.

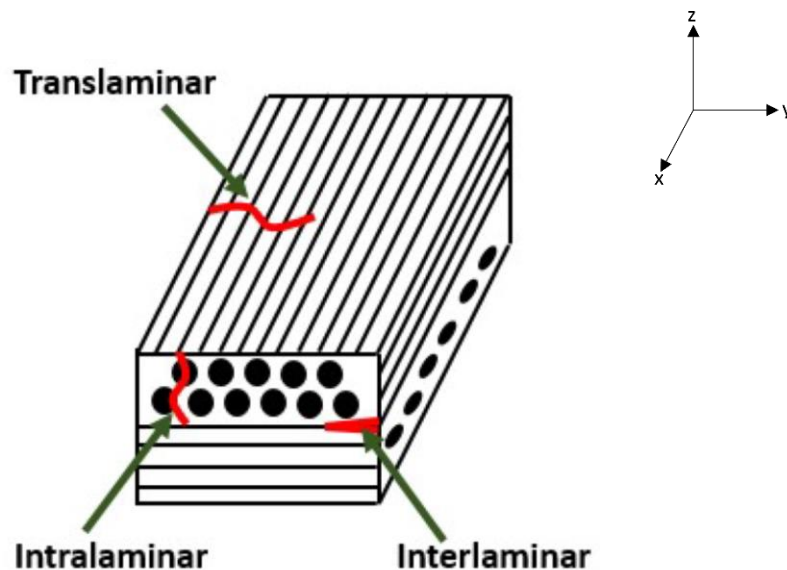


Figure 2.2 Illustration of translaminar, intralaminar and interlaminar fracture modes (Grove and Smith, 1987)

The fiber-reinforced composite compressive failure occurs with the fracture that is not normal to the load direction and the areas of fracture continue to carry load even after failure. In real structures, multidirectional fiber-reinforced composites are utilized where the  $0^0$  plies convey the greater part of the load in a composite laminate (Khandan et al., 2012). Multi directional composite consist of several unidirectional

laminate which are stacked at different angle. A thorough understanding of the failure mechanisms for unidirectional laminates is very important and serves to understand the compressive performance of multi-directional composites. Therefore, a concise outline on the compressive failure in unidirectional fiber-reinforced composites is given in this section.

### **2.3.1 Fiber and matrix failures**

The principle failure mechanisms which may occur independently or all at once during compressive load in unidirectional composites are summarized as follows:

Fiber failure

- *Elastic microbuckling.* This is a term used to describe the shear buckling instability of the matrix with just a small degree of deformation. Besides, lateral displacement across the failure zone is unnoticeable (see Figure 2.3a).
- *Plastic microbuckling or kinking.* This is the term used to define a large non-linear deformation of the matrix due to shear instability. There is a clear displacement across the failure zone which fiber fracture at two points (see Figure 2.3b)
- *Fiber shear failure.* Failure occurs at the fiber level due to a shear instability for example buckling within the fiber, internal defects or flaws at the surface of the fibers (see Figure 2.3c)

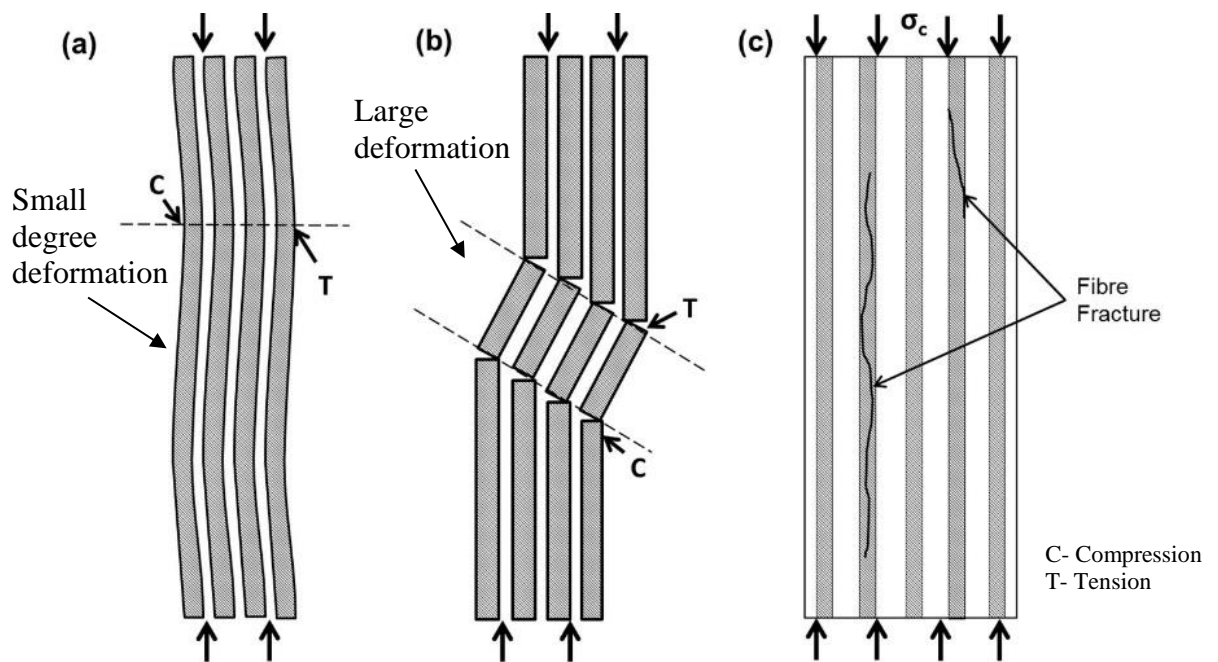


Figure 2.3 Fiber failure modes: (a) Elastic microbuckling; (b) Kinking and (c)

Fiber fracture (Tsampas, 2013)

Matrix failure or fiber/matrix interface failure

- *Ply splitting*. The matrix fractures parallel to the main axial fiber direction (see Figure 2.4a) or propagate rapidly across the ply (see Figure 2.4b and c)
- *Shear band formation*. Matrix yield and fracture occurs in a band oriented at around  $45^\circ$  with respect to the loading direction (see Figure 2.4d)

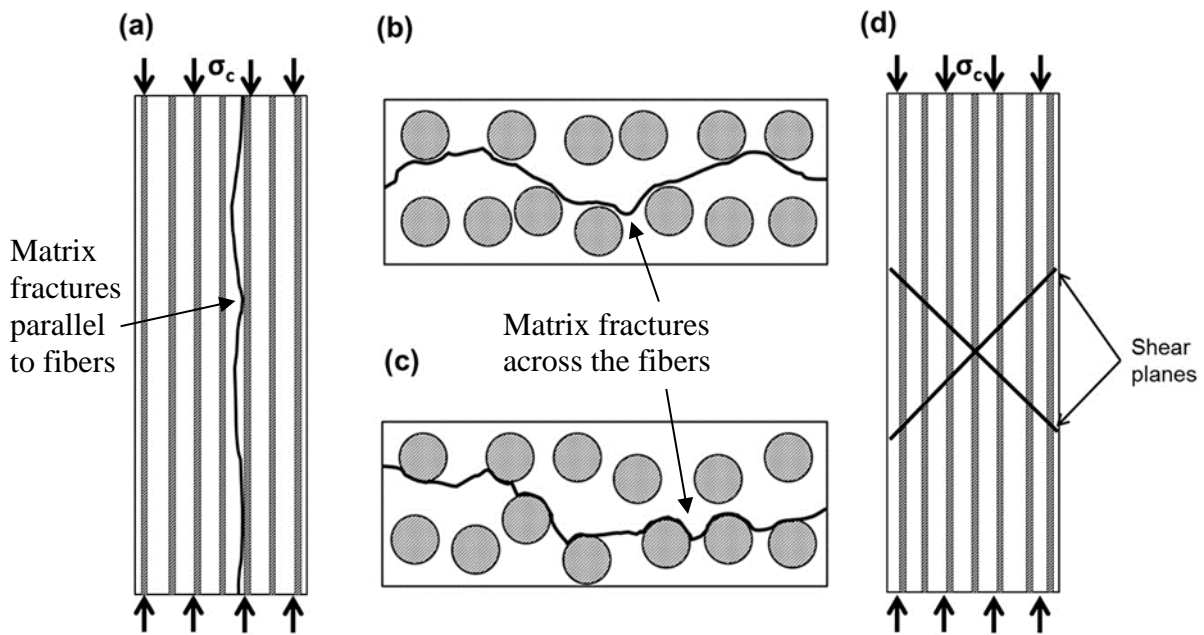


Figure 2.4 Matrix and fiber/matrix modes; (a) Longitudinal ply splitting; (b) and (c) Ply splitting in the laminate plane; (d) Shear band formation (Tsampas, 2013)

### 2.3.1(a) Fiber failure

#### (i) Elastic microbuckling

Fibers are microbuckled elastically while the matrix remains in the elastic region. This type of failure usually happens for low fiber volume fraction (Lee and Waas, 1999b). Here, single continuous long fibers act as slender columns which are supported on an elastic base throughout their length. When fibers are compressed above the threshold, they therefore buckle at relatively low values of external compressive load because of the lack of transverse support from the matrix, as its shear and Young's modulus are very low compared to fibers. In these circumstances the fibers are microbuckled while the matrix remains elastic.

According to Greszczuk (1972), there are several imperfections that can also promote the creation of a microbuckling such as defects at the fiber/matrix interface,

fiber misalignment, residual stresses, porosity and fiber waviness. Greszczuk (1982) additionally proposed that the modulus of the matrix could prompt diverse failure mechanisms, for example, ply splitting (moderate modulus) or compressive fiber failure (high modulus). Specifically, it has been accounted for in the writing that even a little starting fiber misalignment ( $2-3^0$ ) could lower the compressive quality (Wisnom, 1990; Wisnom, 1993).

(ii) Plastic microbuckling/Kinking

Microbuckling of fibers are normally followed by matrix yielding and debonding. The matrix that holds up structure in transverse direction becomes important when fiber content is comparatively high as a result of the composite transverse modulus is considerably larger than the matrix material. Because of that, the matrix begins to yield, and the matrix interface is subsequently debonded or matrix material microcracked. When microcracking or debonding takes place in the matrix, the lateral support in the matrix is lost. Thus, plastic microbuckling happens. Severity of a kink band increases until fiber fracture takes place at two points (Pinho, 2005) when the compressive loading increases. The adjacent fibers can either hinge in a kind of cooperative or independently of each other in the unidirectional composite under compression. Kinking failure is found in a band over the specimen in which large quantities of fibers are rotated and the matrix is subjected to major shear defects.

Kinking arises in a short interval and commonly is cataclysmic in light of the fact that it is started by fiber break, localized fiber microbuckling or shearing of the matrix. The load is then all of a sudden redistributed around the imperfection which causing over-burden to the matrix and henceforth permanently distorted at the broken fiber positions (Argon, 1972; Pinho, 2005).

The understanding on the initiation of fiber micro-buckling/kinking varies among researchers. This is due to the lack of experimental observation of the failure onset caused by the sudden and catastrophic nature of instability type of failure. Post-failure examination is not a reliable method to validate the sequence of events giving rise to the onset of failure. Moreover, it is challenging to arrest the initiation stage of failure (Budiansky and Fleck, 1994).

Kink band boundary angle plays an important role to justify whether or not kinking is a result of microbuckling. It is expected that kink band limit to be at the plane with the highest bending stresses or normal to the loading axis if kinking is the end result of microbuckling. In Figure 2.5, this would mean a zero-kink band angle,  $\beta$ . In contrast, it is discovered that most of the time  $\beta$  lies in the range of  $(30-45^\circ)$  (Chaplin, 1977; Schultheisz and Waas, 1996). The comparability between kink and shear bands might actually suggest that shear is the main factor triggering the development of kink bands. In such cases, kink bands in the planes of maximum shear stress are expected to occur.

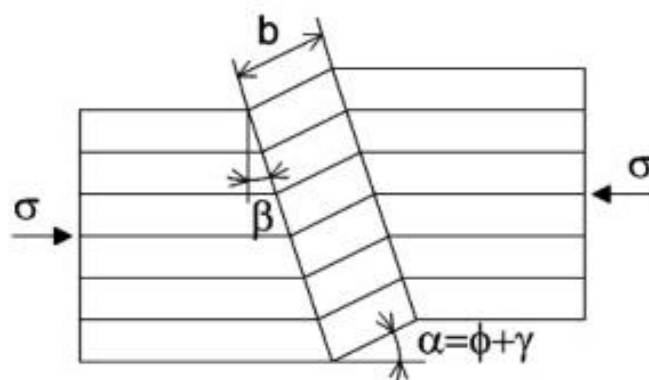


Figure 2.5 Geometry of a kink band

Manufacturing imperfections such as fiber misalignment and ply splitting (matrix cracking) are suggested by Schultheisz and Waas (1996) to be the main culprits

that causing the formation of kinking band and not by fiber fracture as Hahn and Williams (1986) and Chaudhuri (1991) had suggested. With the same opinion, Pinho (2005) also agreed that ply splitting is the mechanism which initiates the kink band formation and not fiber microbuckling.

A region of ply splits develops prior to the kink band formation. The shear strength of the matrix and the fiber/matrix interface strength are the two main properties which directive the compressive performance of the composite (Guild et al., 1989; Pinho, 2005). Fiber diameter, fiber volume fraction and fiber/matrix interfacial toughness are thought to influence the formation of the kink band in some studies (Lee et al., 2000; Yerramalli and Waas, 2004). However, there has been no experimental validation to justify the kinking/splitting interaction mechanism explained based on the parameters that has been modelled.

The progression of kink band formation can be divided into three events as suggested by Pimenta et al. (2009) as shown in Figure 2.6. To begin with, due to the fiber misalignment, bending of the fibers and shearing of the matrix have been induced. When the peak load is reached, the matrix is then yielded, and the fibers start to rotate in a narrow band. Lastly, the fibers failed once the failure strength was reached at which the kink band had been fully defined and ultimate failure had occurred.

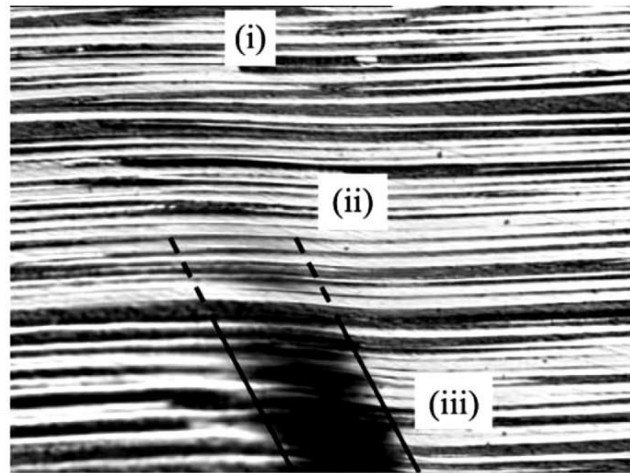


Figure 2.6 Stages of fiber kinking (loaded), (i) elastic domain; (ii) softening domain; (iii) fiber failure domain (Pimenta et al., 2009)

Study on the longitudinal compressive failure in unidirectional composites by Pimenta et al. (2009) identified the sequences of failure mechanisms which result in the collapse of the laminate. From the fracture surfaces analysis shown in Figure 2.7, the compressive failure of a notched composite was initiated from a shear driven compression to a kink band formation and above all, ply splitting took a pivotal role in the kink-band formation.

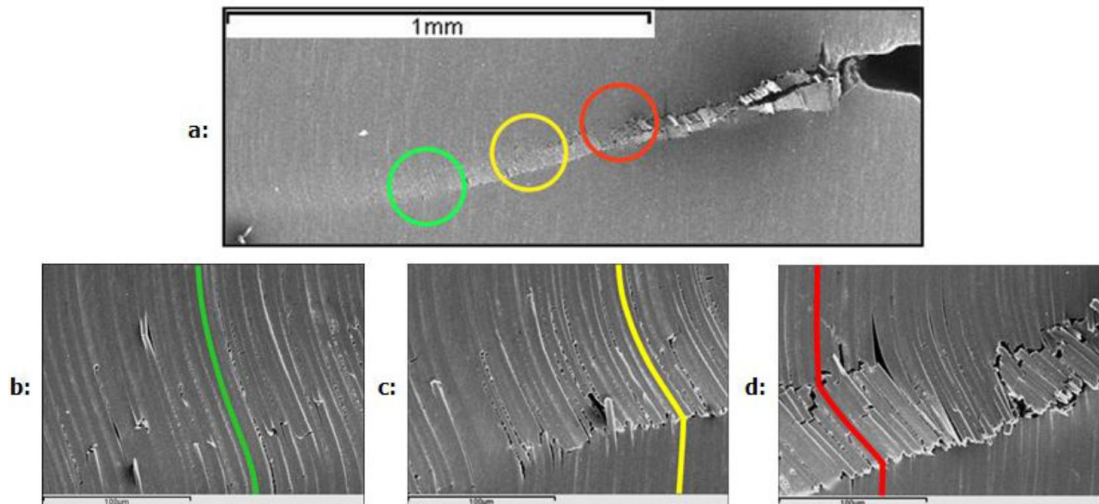


Figure 2.7 (a) Low magnification of a crack propagating from right to left, (b) Initial fiber buckling, (c) Initial cracking, (d) Fully developed kink-band (Pimenta et al., 2009)

Microbuckling can occur either in-plane or out-of-plane in the composite laminates due to the reduction of lateral support from the matrix. The root causes of this failure are the ply splitting, delamination or features such as a notch or free edge (Greenhalgh, 2009).

For the in-plane microbuckling, the reduction of support from the matrix formed a band of microbuckled fibers in the vicinity of a ply split or at the tip of a notch. The in-plane microbuckling does not instantaneously fails since the microbuckled fibers spreads in a stable way. Oppositely, the out-of-plane microbuckling is an unstable failure mechanism that catastrophically fails. It commonly occurs in a load bearing ply when a delamination exists next to it (Greenhalgh, 2009).

### (c) Fiber Fracture

Throughout the literature, fiber failure is identified as an additional and not a dominant compression failure mechanism for unidirectional fiber composite (Fleck and Budiansky, 1991; Gutkin et al., 2010). Normally, this failure occurs when the matrix and fiber/matrix interface are sufficiently strong to obstruct the formation of microbuckling and kinking. Nevertheless, when the fiber strength has exceeded, the failure will occur (Attwood et al., 2015). According to Elices and Llorca (2002), the imperfections along the fiber and at the composite surface could also lead to the fiber fracture as the strength of the fibers have been depreciated.

#### **2.3.1(b) Matrix and fiber/matrix interface failure**

In the following sections, the matrix and fiber/matrix interface failure modes related to compressive failure of composites are presented.

##### (i) Ply splitting

The first form of damage in unidirectional composites is usually matrix microcracks associated with crack development at the fiber/matrix interface (Atkinson and Kiely, 1998; Garg, 1986). Intralaminar failure or ply cracks usually develop in the direction transverse of the ply thickness or parallel to the fibers in that ply due to tensile forces transverse to the fibers or shear forces parallel to the fibers. Indeed, ply splitting is likely to occur in unidirectional composites as a result of the low fiber/matrix interface strength. The growth and the amount of the ply splitting are reliant on several aspects essentially the interfacial fiber/matrix strength, the strength and stiffness of the matrix. In fact, the occurrence of other failure such as delamination would play a part in the development of ply splitting.